Electronic structure and magnetism of amorphous $Co_{1-x}B_x$ alloys

Hiroshi Tanaka and Shinji Takayama
IBM Research, Tokyo Research Laboratory, IBM Japan, Ltd., 5-11, Sanbancho, Chiyoda-ku, Tokyo 102, Japan

Mineshi Hasegawa, Toshiharu Fukunaga, and Uichiro Mizutani
Department of Crystalline Materials Science, Nagoya University, Furo-cho, Chikusa-ku, Nagoya 464-01, Japan

Asaya Fujita and Kazuaki Fukamichi
Department of Materials Science, Tohoku University, 2-1-1, Katahira, Aoba-ku, Sendai 980, Japan
(Received 10 July 1992)

The electronic structure of amorphous $Co_{1-x}B_x$ ($x=0.17$, 0.23, and 0.32) alloys were calculated to clarify their magnetism and electronic specific heat. The electronic structures were calculated self-consistently, both in the spin-polarized and paramagnetic states, by employing the most-localized linear muffin-tin orbital method together with the recursion method. B s and p states split into bonding and antibonding states, and B p states, in particular, hybridize with the tails of Co d states. The exchange splitting of Co d states decreases with increasing B content mainly because of the enhancement of the hybridization. As a result, amorphous Co-B alloys become less ferromagnetic as their B content increases. The calculated magnetic moments per Co atom are proportional to the exchange splitting of Co d states, and decrease with increasing B content. They can be satisfactorily explained by the generalized Stoner model, and agree quantitatively with the experimental data. The density of states at the Fermi level rises with increasing B content, because the highest peak of the minority Co d states shifts toward the Fermi level owing to the decrease in the exchange splitting. This explains a gradual increase in the electronic specific coefficient observed in the experiment.

I. INTRODUCTION

Amorphous $Co_{1-x}B_x$ alloys can be easily formed by rapid quenching techniques in the range $0.16 \leq x \leq 0.35$,[1] and exhibit a typical ferromagnetism in these B contents. Their magnetic properties have been studied extensively. The magnetic moment per Co atom increases with increasing Co content.[2,3] Małozemoff *et al.* proposed a general Slater-Pauling model to explain the changes in the magnetic moment.[4] The Curie temperature T_c and spin-wave stiffness constant also increase with increasing Co content[3] Furthermore, recent experimental data suggest that the Curie temperature of pure amorphous Co should be about 450 K higher than that of crystalline hcp Co.[5] This enhancement of the Curie temperature is explained by the changes in the electronic structures originating from a structural disorder in the amorphous phase.[6,7] In contrast, the Curie temperature of an Fe-B alloy starts to decrease beyond 70 at. % Fe.[8,9] The spin-wave stiffness constant also decreases with an increase in the Fe content from 76 to 88 at. % Fe.[10–12] These facts indicate that the ferromagnetism of amorphous Fe-B alloys become weak toward a pure amorphous Fe limit, whereas that of amorphous Co-B alloys tend to become strong toward a pure amorphous Co limit.

Corresponding to these differences in the magnetic properties, the electronic specific heat coefficient γ_e of amorphous Co-B alloys behave differently from that of amorphous Fe-B alloys.[13] The γ_e for amorphous Co-B alloys increases, whereas that for amorphous Fe-B alloys decreases with an increase in the B content.

To understand the magnetism and electronic specific heats of these materials, it is necessary to determine their electronic structures. There have been several reports on electronic-structure calculations for amorphous Fe-B alloys,[14–17] but few for amorphous Co-B alloys. In the work described here we calculated the electronic structures of amorphous $Co_{1-x}B_x$ alloys ($x=0.17$, 0.23, and 0.32) systematically by using the most localized linear muffin-tin orbital (LMTO) method together with the recursion method.[15] The magnetism and electronic specific heats of the amorphous Co-B alloys are discussed on the basis of the calculated electronic structures.

II. CALCULATIONS

To calculate the electronic structure of an amorphous alloy, it is necessary to construct an atomic-structure model of the alloy. In a metal-metalloid amorphous alloy with a low metalloid content, metalloid atoms are sited in free-volume sites surrounded by metal atoms, so that direct contact between the metalloid atoms is prevented.[18,19] However, some direct contact between metalloid atoms becomes possible beyond a certain critical metalloid content. On the basis of structure analysis data, Waseda estimated this critical metalloid content to be 18 to 20 at. % for metal-boride amorphous alloys.[20]

Taking the above fact into account we constructed atomic-structure models for amorphous $Co_{83}B_{17}$, $Co_{77}B_{23}$, and $Co_{68}B_{32}$ alloys, employing a relaxed dense random

 ©1993 The American Physical Society

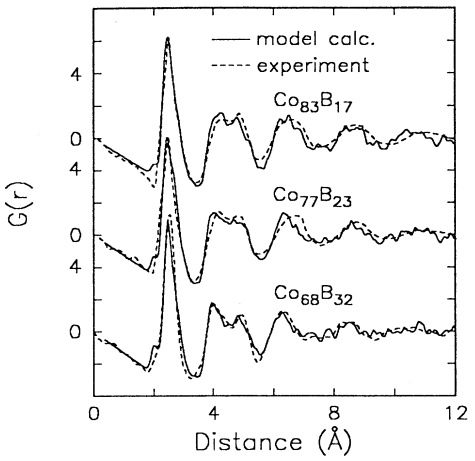

FIG. 1. Comparison of the reduced radial distribution function $G(r)$ for the model atomic structures and experimental ones. The experimental data for the amorphous $Co_{83}B_{17}$ and $Co_{77}B_{23}$ alloys were taken from Ref. 22.

packing of hard spheres (DRPHS) model.[21] First, we constructed a cluster containing 1500 atoms by using the DRPHS model. In this process, B atoms were packed so that they were not in direct contact with each other up to 20 at. %. The remaining B atoms beyond 20 at. % were packed randomly without using this condition. Therefore, there were no direct contacts between the B atoms in the atomic cluster for the $Co_{83}B_{17}$ amorphous alloy, whereas there were some direct contacts between B atoms in the atomic cluster for the $Co_{77}B_{23}$ and $Co_{68}B_{32}$ amorphous alloys. The atomic-structure models for the amorphous alloys were then obtained by relaxing the clusters, using truncated Morse-like pair potentials. The nearest-neighbor distances in the pair potentials were chosen from the experimental data.[22] The depths, widths, and truncation points of the pair potentials were determined in the way described in Ref. 21. In Fig. 1, the reduced radial distribution functions (RDF) $G(r)$ calculated from the atomic-structure models are compared with those obtained experimentally. The experimental data for the amorphous $Co_{83}B_{17}$ and $Co_{77}B_{23}$ alloys were taken from Ref. 22. On the whole, the $G(r)$'s calculated from the model structure agree well with the experimental ones.

On the basis of the atomic-structure models obtained above, we calculated the electronic structures of amorphous $Co_{1-x}B_x$ alloys self-consistently. We employed the most localized LMTO-atomic sphere approximation (ASA) method together with the recursion method.[15] Madulung constants were calculated from the reduced RDF obtained above. We employed a local spin-density functional (LSDF) theory within a scalar relativistic approximation in the form suggested by Barth and Hedin.[23]

III. RESULTS

Figure 2 shows the total and projected densities of states (DOS's) for the $Co_{83}B_{17}$ amorphous alloy. The zero energy level is the Fermi level. There are some common features with the DOS's of Fe-P (Ref. 14) or Fe-B (Refs. 14–17) amorphous alloys. The projected DOS's of Co d states have a two-peak structure. The majority Co d state is mostly occupied and its DOS at the Fermi level is much smaller than that of the minority Co d state. This reflects the fact that amorphous Co-B alloys show strong ferromagnetism. B s and p states split into bonding and antibonding states. In particular, B p states have amplitudes around -8 eV below the Fermi level and around 2–4 eV above the Fermi level. They hybridize with the tails of Co d states. This hybridization plays a significant role in the magnetic properties of the alloys, which we

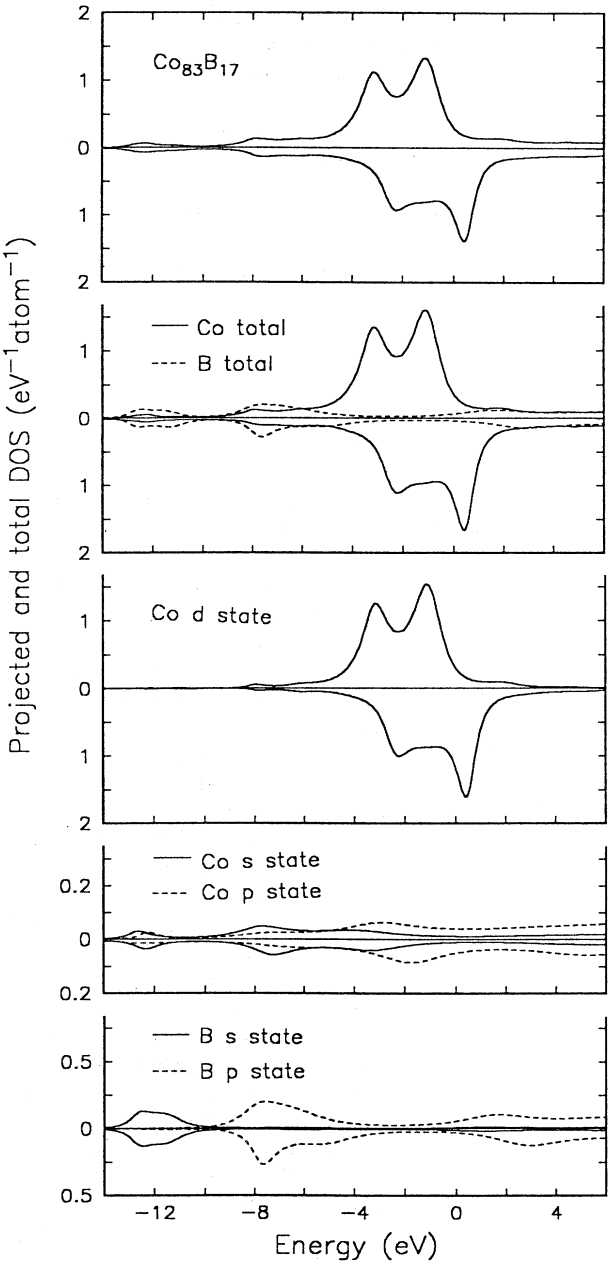

FIG. 2. Total and projected DOS's of amorphous $Co_{83}B_{17}$ alloy. The zero energy level is the Fermi level.

will discuss later. The bonding B s states have an amplitude at deep energy levels (around -12 eV below the Fermi level). The bottoms of the Co s and p states shift toward the low-energy side relative to those in a pure amorphous Co,[7] because Co s and p states hybridize with these deep B s states.

In Fig. 3 we compare the projected DOS's of Co d states for amorphous $Co_{83}B_{17}$, $Co_{77}B_{23}$, and $Co_{68}B_{32}$ alloys. The DOS for pure amorphous Co (Ref. 7) is also included in the figure for comparison. The bandwidth of Co d states becomes narrower with an increase in the B content. This can be attributed to the decrease in the coordination number of Co-Co pairs with increasing B content. We estimated the coordination number by integrating the partial RDF for Co-Co pairs obtained from the model structure up to the first minimum beyond the first peak. The obtained Co-Co coordination numbers are

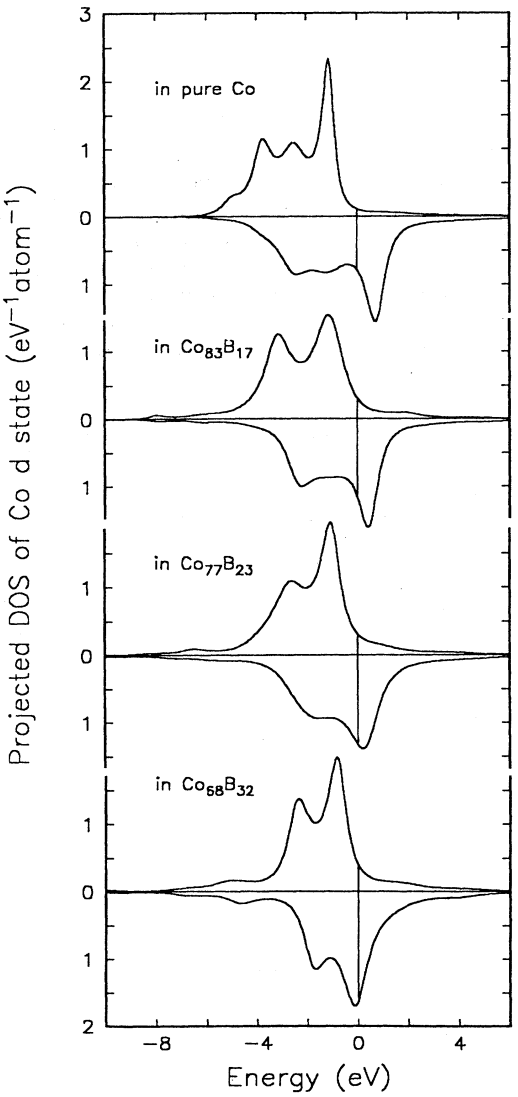

FIG. 3. Projected DOS's of Co d states for amorphous pure Co (Ref. 7), $Co_{83}B_{17}$, $Co_{77}B_{23}$, and $Co_{68}B_{68}$ alloys. The zero energy level is the Fermi level.

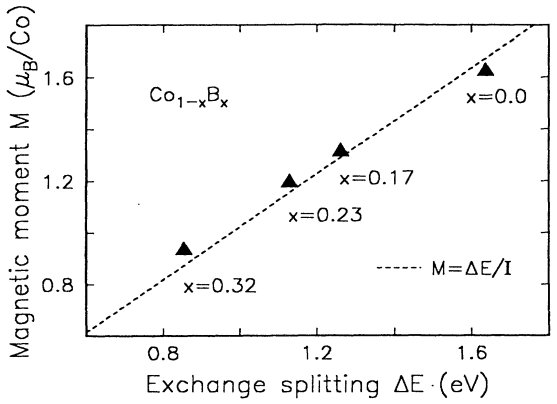

FIG. 4. Calculated magnetic moments M as a function of exchange splitting of Co d states ΔE. The dashed line corresponds to $M=\Delta E/I$ with $I=0.979$ eV, which is predicted by the generalized Stoner model. (Ref. 25).

12.2 for $Co_{83}B_{17}$, 11.9 for $Co_{77}B_{23}$, and 10.7 for $Co_{68}B_{32}$ amorphous alloys. Although this estimation scheme tends to overestimate the coordination number in general,[24] the general trend is obviously for the Co-Co coordination number to decrease with an increase in the B content. Note that the exchange splitting of Co d states ΔE decreases with an increase in the B content. Corresponding to this, the highest peak of the minority d states shifts close to the Fermi level, though that of majority d states generally stays around -1 eV below the Fermi level. The DOS at the Fermi level increases with an increase in the B content because of the shift of the minority-spin band.

The electron occupation number for each state and the resulting magnetic moment for each atom are listed in Table I. The magnetic moment per Co atom decreases with increasing B content in the same way that the exchange splitting of Co d states ΔE decreases. The value of ΔE for Co d states can be evaluated from the energy difference of the band center potential parameters C_d for the majority and minority Co d states, which were obtained from the electronic structure calculations. In Fig. 4 we plotted the magnetic moments per Co atom obtained from the present electronic-structure calculations (triangle symbols) as a function of ΔE. The dashed line indicates changes in the magnetic moment estimated by the generalized Stoner model.[25] According to this model, the magnetic moment M is proportional to the exchange splitting ΔE, and can be estimated by the equation

$$M=\Delta E/I\ , \tag{1}$$

where I is the Stoner parameter and 0.979 eV for Co.[26] As shown in the figure, the magnetic moment of amorphous Co-B alloys can be satisfactorily explained by the generalized Stoner model.

IV. DISCUSSION

Recently, Mizutani *et al.*[27] investigated systematically the magnetism, electronic properties, and low-

TABLE I. Electron occupation numbers of each state and resulting magnetic moments for amorphous $Co_{1-x}B_x$ alloys with $x=0.17$, 0.23, and 0.32. Those for pure amorphous Co (Ref. 7) are also listed for comparison.

System	Atom	Spin	s	p	d	$M(\mu_B)$	Total
Co	Co	Up	0.31	0.39	4.62	1.63	9.00
		Down	0.36	0.45	2.88		
$Co_{83}B_{17}$	Co	Up	0.33	0.40	4.50	1.32	9.14
		Down	0.36	0.45	3.10		
	B	Up	0.35	0.79		−0.04	2.32
		Down	0.37	0.81			
$Co_{77}B_{23}$	Co	Up	0.35	0.42	4.43	1.18	9.22
		Down	0.35	0.46	3.21		
	B	Up	0.40	0.77		0.01	2.33
		Down	0.39	0.77			
$Co_{68}B_{32}$	Co	Up	0.36	0.46	4.31	0.94	9.32
		Down	0.34	0.49	3.36		
	B	Up	0.41	0.75		−0.01	2.33
		Down	0.40	0.77			

temperature specific heats of amorphous $(Co_{0.85}B_{0.15})_{100-x}X_x$ (X = B, Al, Si, and V) alloys (in a publication hereafter referred to as paper II). In this paper we discuss the magnetism and electronic specific heats of amorphous $Co_{1-x}B_x$ alloys on the basis of their experimental data and our own calculated electronic structures. Their experimental data on the saturation magnetizations M, Curie temperatures T_c, spin-wave stiffness constants D, and Debye temperature θ_D for amorphous $Co_{1-x}B_x$ alloys are summarized in Table II so that they can be conveniently referred to during our later discussion.

A. Magnetism

The calculated magnetic moments per Co atom are compared with the experimental ones[27,28] in Fig. 5. The results agree well, and decrease with increasing B content. In general, the magnetic moment per TM atom decreases with an increase in the metalloid content in amorphous TM-metalloid alloys. A simple explanation is provided by the interatomic charge-transfer model, which attributes this decrease of magnetic moment to the interatomic charge transfer from metalloid atoms to TM minority d states, resulting in the band-filling effect.[29] On the other hand, Alben *et al.*[30] and Allen *et al.*[31] suggested that the suppression in the magnetic moment resulted from a loss of d character due to the chemical bonding between TM d states and metalloid p states, but not from the interatomic charge transfer. The present calculations support their explanation as discussed below. According to our results, the charge transfer from a B atom is almost constant ($\sim$0.68 electrons) regardless of the B content (see Table I), and too small to explain the decrease in the magnetic moment. The intra-atomic charge transfer from the Co majority d state to the minority d state reduces the magnetic moment per Co atom more significantly than the interatomic charge transfer, as shown in Table I. The intra-atomic charge transfer comes from the decrease in the exchange splitting of Co d states with increasing B content, as mentioned before.

TABLE II. Saturation magnetization μ, spin-wave stiffness constant D, Curie temperature T_c, and Debye temperatures θ_D for amorphous $Co_{1-x}B_x$ alloys. The Curie temperatures for 15 at. % B, 19.75 at. % B, and 23.50 at. % B samples could not determined, because they exceeded the crystallization temperatures.

Composition (at. % B)	M (μ_B/Co)	D (meV Å^2)	T_c K	θ_D K
15.00	1.36	525		456
19.75	1.12	420		390
23.50	1.04	279		400
27.75	0.92	208	670	433
32.00	0.74	166	490	408
36.25	0.50	100	290	395

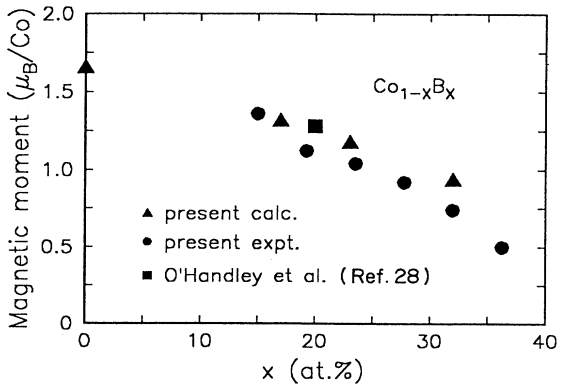

FIG. 5. The magnetic moments per Co atom obtained from the present electronic-structure calculations (solid triangles) are compared with experimental ones [solid circles (Ref. 27) and solid square (Ref. 28)].

Therefore, the magnetic moment decreases because of the decrease in the exchange splitting rather than the interatomic charge transfer.

The spin-wave stiffness constant and Curie temperature also decrease with increasing B content. In order to study the effect on the magnetism of adding B atoms, we also calculated the electronic structure in the *paramagnetic* state. Figure 6 shows the calculated total DOS's of a Co site (solid line) and a B site (dashed line) for the amorphous $Co_{83}B_{17}$, $Co_{77}B_{23}$, and $Co_{68}B_{32}$ alloys, respectively. The total DOS for a pure amorphous Co is also shown in the figure for comparison. The bandwidth of the Co DOS decreases with increasing B content as is the case with the spin-polarized calculations, because the coordination number of Co-Co pairs decreases. The B p states split into bonding and antibonding states, and have amplitudes around $-8\sim-6$ eV below the Fermi level and $2\sim4$ eV above the Fermi level. They hybridize with the Co d states, and the tails of the Co d states are

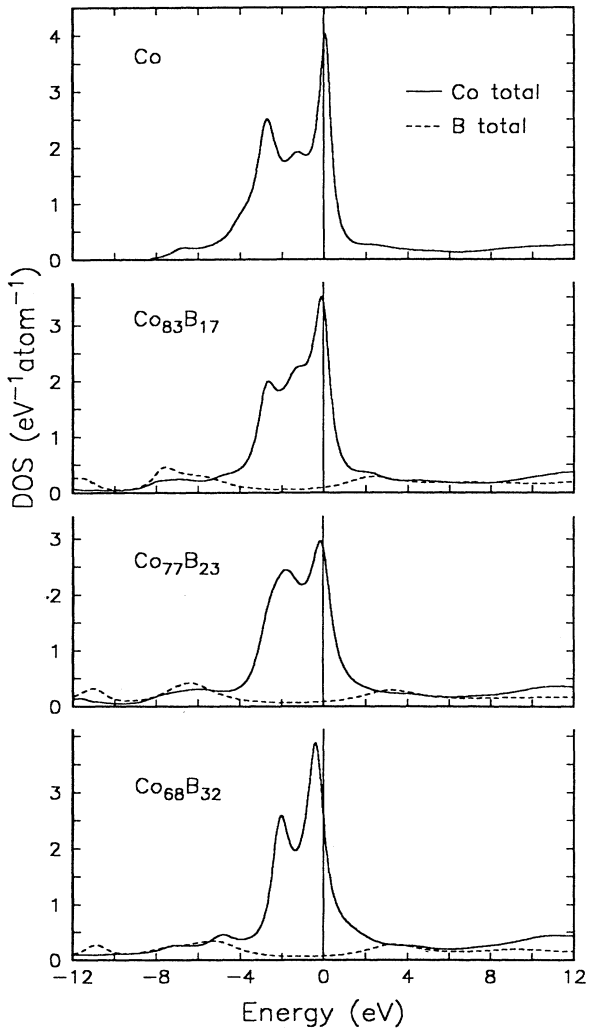

FIG. 6. Paramagnetic DOS's of Co and B sites for amorphous $Co_{83}B_{17}$, $Co_{77}B_{23}$, and $Co_{68}B_{68}$ alloys. The total DOS of pure amorphous Co (Ref. 7) is also plotted for comparison. The zero energy level is the Fermi level.

enhanced as the B content increases. Consequently, the amplitude of the highest peak of the Co DOS is suppressed up to 23 at. % B. On the other hand, the band-narrowing effect is superior to the effect of hybridization in 32 at % B, so that the amplitude of the highest peak of the Co DOS starts to increase. At the same time, the peak shifts toward the low-energy side with increasing B content because of the hybridization. The DOS at the Fermi level decreases for 17 at. % and 23 at. % B in this order because of the suppression of the highest peak of the Co DOS. In the case of 32 at. % B, a shift of the highest peak away from the Fermi level becomes substantial and is responsible for a decrease in the Co DOS at the Fermi level. Although various factors are involved, the *paramagnetic* DOS at the Fermi level decreases consistently with increasing B content as a result of the hybridization between the Co d states and B p states. This decreases the exchange energy of a Co atom, resulting in the above-mentioned decrease in the exchange splitting. However, the Stoner criterion is satisfied even in the amorphous $Co_{68}B_{32}$ alloy, indicating that the alloy is ferromagnetic.

B. Electronic specific heat

In paper II, the low-temperature specific heats $C(T)$ were measured for amorphous $Co_{1-x}B_x$ alloys to determine the DOS's at the Fermi level experimentally. The experimental data were analyzed on the basis of the spin-wave approximation by using the following equation:

$$C(T)=\gamma_e T+\alpha_l T^3+C_m(T)\ , \tag{2}$$

with

$$C_m(t)=\sigma_s T^{3/2}+\sigma_n T^{-2}\ , \tag{3}$$

where γ_e is the electronic, α_l the lattice, σ_s the spin-wave, and σ_n the nuclear specific heat coefficients. The electronic specific-heat coefficient reflects the DOS at the Fermi level through the equation

$$\gamma_e=\tfrac{1}{3}(1+\lambda)\pi^2 k_B^2 n(E_F)\ , \tag{4}$$

where λ and $n(E_F)$ are the electron-phonon coupling constant and the DOS at the Fermi level, respectively. The Debye temperature was evaluated from the obtained lattice specific heat coefficient α_l through the well-known equation

$$\alpha_l=\tfrac{12}{5}\pi^4 k_B N_A \theta_D^{-3}\ , \tag{5}$$

where N_A is Avogadro's number. The obtained Debye temperatures are also listed in Table II.

To evaluate γ_e from the present electronic-structure calculations, it is necessary to estimate the electron-phonon coupling constant λ. For this purpose we employed a rigid muffin-tin approximation (RMTA).[32] The approximation was proposed by Gomersall and Gyorffy, and parametrized within the atomic-sphere approximation (ASA) by Skriver and Mertig.[33] According to McMillan,[34] λ can be described in the form

$$\lambda=\frac{\eta}{M\langle\omega^2\rangle}\ , \tag{6}$$

where η is the Hopfield parameter, M the atomic mass, and $\langle\omega^2\rangle$ the average phonon frequency. The Hopfield parameter can be calculated by employing the RMTA on the basis of the electronic structures and wave functions calculated above, while $\langle\omega^2\rangle$ has to be estimated from experiments. We estimated $\langle\omega^2\rangle$ from the Debye temperature by using the well-known relation $\langle\omega^2\rangle^{1/2}=0.69\theta_D$. We used a Debye temperature of 417 K, which was obtained by averaging the experimental data listed in Table II. This is because the experimental data are scattered in the range from 390 to 456 K. The calculated values of λ are 0.12 ± 0.02 for pure amorphous Co, 0.29 ± 0.06 for $Co_{83}B_{17}$, 0.39 ± 0.08 for $Co_{77}B_{23}$, and 0.33 ± 0.07 for $Co_{68}B_{32}$. The figures after the $\pm$ sign correspond to the uncertainty of the experimental Debye temperature. Now, we can estimate the γ_e from the present electronic structure calculations by substituting these values into Eq. (4).

In Fig. 7, experimental γ_e's are compared with theoretical ones. γ_e for the crystalline hcp Co is also plotted in the figure. Although the experimental values are higher than the theoretical ones, which need further study, both increase with increasing B content. This increase in γ_e stems from the increase in the *spin-polarized* DOS at the Fermi level with increasing B content (see Fig. 2). The DOS increases with increasing B content because of the decrease in the exchange splitting of Co d states, as mentioned before. The experimental γ_e, however, keeps increasing even beyond 30 at. % B, whereas theoretical one tends to reach saturation around this B content. The rapid increase in γ_e beyond 30 at. % B is expected to result from weakening of the ferromagnetism. As shown in Table I, the spin-wave stiffness constant decreases with increasing B content, which indicates that amorphous Co-B alloy becomes less magnetic with increasing B content. For weak or unstable ferromagnetic materials, the magnetic specific heat $C_m(T)$ is described by

$$C_m(T)=A+\gamma_m T+\alpha_m T^3\ , \tag{7}$$

rather than Eq. (3),[35] and the total specific heat can be described in the form

$$C(T)=A+(\gamma_e+\gamma_m)T+(\alpha_l+\alpha_m)T^3\ . \tag{8}$$

The electronic specific-heat coefficient γ_e then cannot be distinguished from the magnetic specific-heat coefficient γ_m, because both of them have the same temperature dependence. In fact, it was observed that the linearly temperature-dependent specific heat coefficients were significantly enhanced by the magnetic contribution in amorphous Co-Zr-X (X=Si, Ge, Zr, Al) and Co-B-X (X=Al, Si, and V) alloys when their spin-wave stiffness constants were less than about 150 meV Å (see paper II). Note that the spin-wave stiffness constants of amorphous $Co_{68}B_{32}$ and $Co_{64}B_{36}$ alloys are 166 meV Å and 100 meV Å, respectively (see Table II). Figure 8 shows the total DOS's (the sum of the DOS's in the majority and minority spin states) for the amorphous pure Co,[7] $Co_{83}B_{17}$, $Co_{77}B_{23}$, and $Co_{68}B_{32}$ alloys. Note that the Fermi level falls near a local minimum of the total DOS in each of the first three amorphous metals, whereas it falls on a slope of the total DOS in the $Co_{68}B_{32}$ alloy. This indicates that the ferromagnetism with the collinear spin configuration becomes unstable for the $Co_{68}B_{32}$ alloy with respect to the band energy.

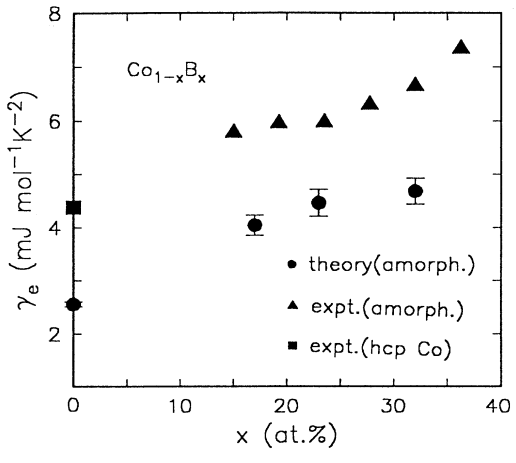

FIG. 7. Comparison of the electronic specific-heat coefficients obtained from the experiments (solid triangles) and those calculated from the electronic structures (solid circles). Note here that the electron-phonon enhancement factor is taken into account in the calculations. Error bars for the calculated data correspond to the uncertainty of the Debye temperature (see text). The experimental value for hcp Co (solid square) is also plotted.

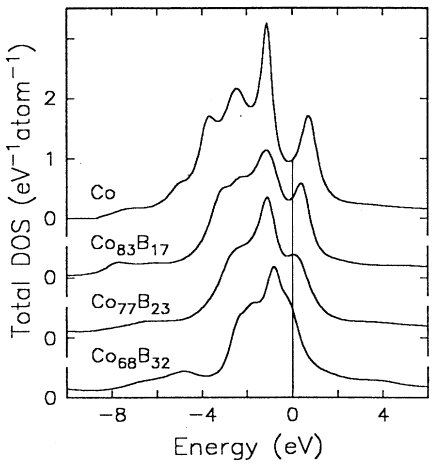

FIG. 8. Total (sum of the majority part and minority part) DOS's for amorphous pure Co (Ref. 7), $Co_{83}B_{17}$, $Co_{77}B_{23}$, and $Co_{68}B_{68}$ alloys. The zero energy level is the Fermi level.

V. CONCLUSION

The magnetism and electronic specific heats of amorphous Co-B alloys were studied in relation to their electronic structures. The electronic structures calculated

self-consistently indicate that amorphous $Co_{1-x}B_x$ alloys are ferromagnetic at least in the range $x \leq 0.32$. The magnetic moment per Co atom and the exchange splitting of Co d states decrease with increasing B content. This degradation of the ferromagnetism results from the hybridization between the B p states and Co d states, and the resulting change in the electronic structures. The calculated magnetic moments agree quantitatively with experimental ones. They change in proportion to the exchange splitting of Co d states, and are satisfactorily explained by the generalized Stoner model. The DOS at the Fermi level increases with increasing B content, because the exchange splitting of Co d states decreases and the main peak of the minority Co d state shifts toward the Fermi level. Correspondingly, the electronic specific-heat coefficient increases with increasing B content.

[1]R. Hasegawa and R. Ray, J. Appl. Phys. **49**, 4174 (1978).
[2]R. Hasegawa and R. Ray, J. Appl. Phys. **50**, 1586 (1979).
[3]H. Watanabe, H. Morita, and H. Yamaguchi, IEEE Trans. Magn. **MAG-14**, 944 (1978).
[4] A. P. Malozemoff, A. R. Williams, and V. L. Moruzzi, Phys. Rev. B **29**, 1620 (1984).
[5]K. Fukamichi, T. Goto, and U. Mizutani, IEEE Trans. Magn. **MAG-23**, 3590 (1987).
[6]Y. Kakehashi, Phys. Rev. B **43**, 10 820 (1991).
[7]H. Tanaka and S. Takayama, J. Phys.: Condens. Matter **4**, 8203 (1992).
[8]C. L. Chien and K. M. Unruh, Phys. Rev. B **24**, 1556 (1981).
[9]T. Stobiecki, IEEE Trans. Magn. **MAG-18**, 780 (1982).
[10]N. S. Kazama, M. Mitera, T. Masumoto, in *Proceedings 3rd International Conference on Rapid Quenched Metals,* edited by B. Canter (Metal Society, London, 1978), Vol. 2, pp. 164–171.
[11]R. Hasegawa and R. Ray, Phys. Rev. B **20**, 211 (1979).
[12]M. Matsuura, U. Mizutani, and Y. Yazawa, J. Phys. F **11**, 1393 (1981).
[13]M. Matsuura and U. Mizutani, J. Magn. Magn. Mater. **31-34**, 1481 (1983).
[14]T. Fujiwara, J. Phys. F **12**, 661 (1982).
[15]T. Fujiwara, J. Non-Cryst. Solids **61&62**, 1039 (1980).
[16]S. Krompiewski, U. Krey, U. Krauss, and H. Ostermeier, J. Magn. Magn. Mater. **73**, 5 (1988).
[17]H. J. Nowak, O. K. Andersen, T. Fujiwara, and O. Jepsen, Phys. Rev. B **44**, 3577 (1991).
[18]J. F. Sadoc and J. Diximer, Mater. Sci. Eng. **23**, 187 (1976).
[19]Y. Waseda, H. Okazaki, and T. Masumoto, Sci. Rep. Inst. Tohoku Univ. **26A**, 202 (1977).
[20]Y. Waseda, Prog. Mater. Sci. **26**, 1 (1981).
[21]T. Fujiwara and Y. Ishii, J. Phys. F **10**, 1901 (1980).
[22]Y. Waseda and H. S. Chen, Phys. Status Solidi A **49**, 387 (1978).
[23]U. von Barth and L. Hedin, J. Phys. C **5**, 1629 (1972).
[24]Y. Waseda, *The Structure of Non-Crystalline Materials* (McGraw-Hill, New York, 1980).
[25]O. K. Andersen, O. Jepsen, and D. Gloetzel, in *Proceedings of the International School of Physics,* Enrico Fermi Course LXXXIX, edited by F. Bassani, F. Fumi, and M. P. Tosi (North-Holland, Amsterdam, 1985), pp. 59–176.
[26]J. F. Janak, Phys. Rev. B **16**, 255 (1977).
[27]U. Mizutani, M. Hasegawa, K. Fukamichi, Y. Hattori, Y. Yamada, H. Tanaka, and S. Takayama, following paper, Phys. Rev. B **46**, 2678 (1993).
[28]R. C. O'Handley, R. Hasegawa, R. Ray, and C.-P. Chou, J. Appl. Phys. **48**, 2095 (1977).
[29]K. Yamaguchi and T. Mizoguchi, J. Phys. Soc. Jpn. **39**, 541 (1975).
[30]R. A. Alben, J. I. Budnick, and G. S. Cargill, in *Magnetic Glasses,* edited by J. J. Gilman and H. L. Leamy (American Society of Metals, Metals Park, Ohio, 1978).
[31]J. W. Allen, A. C. Wright, and G. A. N. Connel, J. Non-Cryst. Solids **40**, 509 (1980).
[32]G. P. Gaspari and B. L. Gyorffy, Phys. Rev. Lett. **28**, 801 (1972).
[33]H. L. Skriver and I. Mertig, Phys. Rev. B **41**, 6553 (1990).
[34]W. L. McMillan, Phys. Rev. **167**, 331 (1968).
[35]S. Kanemaki, O. Takehira, T. Goto, and U. Mizutani, J. Phys.: Condens. Matter **4**, 2217 (1992).